Engineering Structures 248 (2021) 113185

Contents lists available at ScienceDirect

Engineering Structures

journal homepage: www.elsevier.com/locate/engstruct

Seismic performance factors for timber buildings with woodframe shear walls

Xavier Estrella[a,*], Pablo Guindos[a,b,c], José Luis Almazán[b], Sardar Malek[d], Hernán Santa María[b,e], Jairo Montaño[a], Sebastián Berwart[a]

[a] UC Center for Wood Innovation (CIM), Pontificia Universidad Católica de Chile, Av. Vicuña Mackenna, Santiago 7820436, Chile
[b] Department of Structural and Geotechnical Engineering, Pontificia Universidad Católica de Chile, Av. Vicuña Mackenna, Santiago 7820436, Chile
[c] Department of Construction Engineering and Management, Pontificia Universidad Católica de Chile, Av. Vicuña Mackenna, Santiago 7820436, Chile
[d] Department of Civil Engineering, University of Victoria, 3800 Finnerty Rd, Victoria, BC V8P 5C2, Canada
[e] Research Center for Integrated Disaster Risk Management (CIGIDEN), ANID/FONDAP/15110017, Av. Vicuña Mackenna, Santiago 7820436, Chile

ARTICLE INFO

Keyword:
Timber structures
Wood frame walls
Light-frame construction
Seismic performance factors
Mid-rise timber buildings

ABSTRACT

Seismic performance factors are an engineering tool to estimate force and displacement demands on structures designed through linear methods of analysis. In Chile, the NCh433 standard provides the regulations, requirements, and factors for seismic design of several structural typologies and systems. However, when it comes to wood frame structures, previous research has found that the NCh433 provisions are highly restrictive and result in over-conservative designs. Therefore, this paper presents an experimental and numerical investigation aimed at proposing new, less restrictive seismic performance factors for wood frame buildings. Following the FEMA P-695 guidelines and a novel ground motion set for subduction zones, this research embraced: (1) testing of several full-scale specimens, (2) developing of detailed and simplified numerical models, and (3) analyzing the seismic performance of a comprehensive set of structural archetypes. 201 buildings were analyzed and results showed that changing the current NCh433 performance factors from $R = 5.5$ & $\Delta_{max} = 0.002$ to $R = 6.5$ & $\Delta_{max} = 0.004$ decreases the average collapse ratio of wood frame structures by 13.3% but keeps the collapse probability below 20% for all the archetypes under study. Besides, it improves the cost-effectiveness of the buildings and enhances their competitiveness when compared to other materials, since savings of 40.4% in nailing, 15.9% in OSB panels, and 7.3% in timber studs were found for a 5-story building case study. Further analyses showed that the buildings designed with the new factors reached the "enhanced performance objective" as defined by the ASCE 41–17 standard, guaranteeing neglectable structural and non-structural damage under highly recurring seismic events. Finally, dynamic analyses revealed that the minimum base shear requirement C_{min} of the NCh433 standard is somewhat restrictive for soil classes A, B, and C, leading to conservative results compared to archetypes where the C_{min} requirement did not control the structural design.

1. Introduction

Seismic performance factors (SPFs) are a relevant tool when designing modern earthquake-resistant structures. They provide a first approach to estimate strength and displacement demands on structural systems designed with linear elastic methods, but that are expected to behave nonlinearly during moderate to severe earthquakes. Due to their simplicity and ease of use, SPFs represent a simple tool for researchers and practitioners of structural engineering and are included in most seismic standards worldwide. The current state-of-the-art proposes several SPFs for different purposes during the design phase, such as the response modification factor R, the system overstrength factor Ω_0, the deflection amplification factor C_d, or the maximum allowable story drift Δ_{max} [1–3]. However, the most widely used factors in national and international building codes are the R factor and the maximum allowable story drift Δ_{max}.

The design philosophy behind the SPFs relies on the nonlinear deformation capacity of code-compliant buildings. For a given fundamental period T_1, the R factor reduces the design base shear V_s calculated from an elastic design acceleration spectrum Sa_D, as pictured in

* Corresponding author at: UC Center for Wood Innovation (CIM), Pontificia Universidad Católica de Chile, Av. Vicuña Mackenna, Santiago 7820436, Chile.
E-mail address: exestrella@uc.cl (X. Estrella).

https://doi.org/10.1016/j.engstruct.2021.113185
Received 14 April 2021; Received in revised form 9 August 2021; Accepted 8 September 2021

Fig. 1(a). This latter means $V_s(T_1) = W \times Sa_D/R$, where W is the effective seismic mass of the building. The ductility of the structural system determines how much the base shear is reduced; the higher the ductility, the higher the R factor, and the lower the base shear. For instance, the ASCE 7–16 standard [4] defines an R factor equal to 4 for ordinary reinforced concrete shear walls, while for ordinary plain concrete shear walls R is equal to 1.5. The rationale of an R factor which depends on the ductility is allowing the structure to suffer damage during strong earthquakes, but at the same time to assure that a life-threatening performance level is not reached. This way, the cost-effectiveness of the building improves by reducing the cost of the main structural system. Therefore, the R factor determines the relative spectral acceleration that the structure is required to resist to guarantee the resilience of the building. On the other hand, the maximum allowable story drift Δ_{max} provides a means to improve structural performance by controlling the stiffness of the building. As illustrated in Fig. 1(b), it limits the maximum interstory drift for linear elastic designs (under a design spectrum reduced by the R factor), aiming at minimizing the non-structural damage during moderate earthquakes and the structural damage during severe earthquakes.

The quantification of the values adopted for the SPFs is usually based on detailing and expected performance. However, for newly defined or undefined structural systems, they are typically determined employing engineering criteria and qualitative comparisons to achieve an equivalent behavior to that of other code-defined systems. Although a good performance may be achieved for buildings designed using such factors, the lack of a robust and rational methodology to quantify them may lead to over-conservative designs that are not economically competitive in the real estate market.

Nowadays, to design mid- to high-rise buildings in Chile, the current normative stipulates that the requirements of the national standard for seismic design of buildings NCh433 [3] must be met. For wood frame construction, the standard establishes an R factor equal to 5.5, and a maximum allowable story drift Δ_{max} of 0.002 h, where h is the interstory height. This maximum story drift controls the relative displacement of the center of mass of two consecutive stories (for linear elastic designs) and was originally set to guarantee the performance of stiff systems such as reinforced concrete wall structures. However, this requirement may be difficult to achieve by flexible systems such as wood frame buildings, resulting in very rigid structures with short periods and low ductility demands, wasting the inherent advantages of timber construction.

The suitability of the Chilean SPFs regarding wood frame construction can be analyzed by comparing them to those defined in international standards. As discussed by Dolan et al. [5], the American ASCE 7–16 standard [4] defines an R factor equal to 6.5 for light-frame shear walls with wood structural panels. If the differences in the seismic demand (i.e., seismic design spectrum) between both countries are not taken into account, the lower R factor in the NCh433 standard [3] results in wood frame buildings being designed for spectral accelerations 18% higher than equivalent structures designed under the USA requirements. If the different design spectra are considered, the spectral accelerations can be up to 2.75–3.0 times higher [5]. It is also relevant to analyze how other materials are considered with respect to timber in both standards. For instance, the R factors for ordinary reinforced concrete and masonry walls in the ASCE 7–16 standard [4] are 4 and 2, while in the NCh433 [3] standard are 7 and 4, respectively. Therefore, it can be noted that concrete and masonry are required to resist 30% and 225% higher spectral accelerations than timber in the USA, while they are required to resist 21% lower and 25% higher spectral accelerations than timber in Chile, respectively.

Regarding the maximum allowable story drift Δ_{max}, the ASCE 7–16 [4] requirement is 0.00625 h for wood-frame structures 4 stories or less ($\Delta_{max} = \Delta_{adm}/C_d = 0.025h/4 = 0.00625h$), meaning that the Chilean code requires timber buildings to be over 3 times stiffer than similar buildings in the USA. Therefore, the lateral design is mainly controlled by drift restrictions that are difficult to meet in areas prone to high seismic spectral accelerations. The small deflections expected for a Δ_{max} of 0.002 h result in overdesigned wood frame walls; hence, the potential of wood frame constructions is not fully harnessed, as it has been reported by previous researchers. For instance, Santa María et al. [6] reported large cross-sections and sturdy walls while designing a six-story wood frame building according to the current Chilean seismic regulations. Cárcamo et al. [7] highlighted the need to incorporate rigid structures, such as concrete or cross-laminated timber CLT walls, in wood frame buildings in order to meet the maximum drift requirement. Guíñez et al. [8] reported that, at a 0.002 h drift, wood frame walls only reach about 16% to 23% of their maximum strength capacity, showing that these walls allow larger drifts than, for instance, concrete ones. Additionally, a maximum allowable story drift Δ_{max} equal to 0.004 h was recommended by Guíñez et al. [8] for mid-rise timber buildings so that about 40% of the strength capacity of wood frame walls is harnessed.

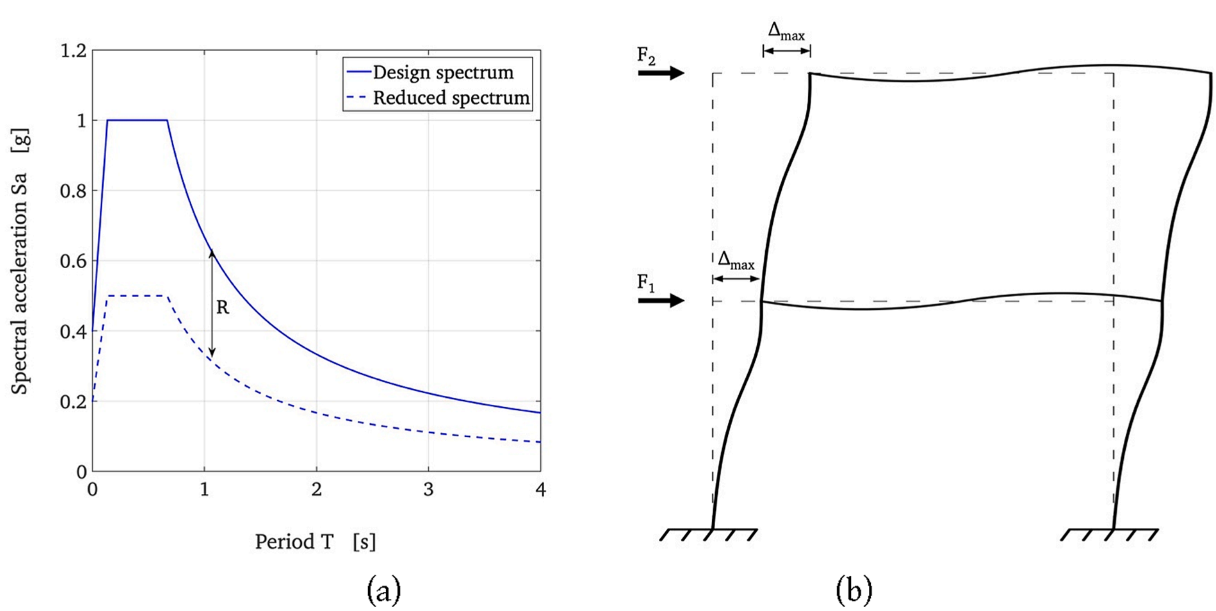

Fig. 1. Seismic performance factors: (a) response modification factor R and reduced design spectrum, and (b) maximum allowable story drift Δ_{max}.

A robust seismic design standard is crucial for the development and growth of timber construction in Chile. However, according to previous research [9], the basis of the SPFs for timber structures in the current Chilean seismic standard is not entirely clear. Therefore, this paper presents the results of a comprehensive research project aimed at validating a new set of seismic performance factors for wood frame buildings through a rational approach. Following the guidelines of the FEMA P-695 methodology [1], this investigation embraced: (1) testing of materials, connections, and wall assemblies, (2) nonlinear numerical modeling of wood frame walls under monotonic and cyclic loads, (3) selection of ground motions for subduction zones, (4) performance evaluation of a comprehensive set of wood frame buildings through 3D nonlinear dynamic analyses, and (5) validation of a new set of SPFs. This project was a collaborative effort of researchers from the Pontifical Catholic University of Chile, the University of Bío-Bío, and the University of Technology Sydney, and the results aim at providing new guidelines towards an efficient seismic design of wood frame buildings.

2. Materials and methodology

This section presents the work conducted on wood frame structures at the first stage of this project, which provided a sound background to support the validation of the new set of SPFs discussed in Section 3. In order to appropriately adapt the FEMA P-695 guidelines [1] to the local Chilean context, different research fields were covered throughout this investigation: experimental tests, computational models, seismological ground motions, architectural designs, structural designs, and three-dimensional dynamic simulations. A brief description of the work carried out in each field is presented in the following paragraphs.

2.1. *Testing program*

Wood is a natural material whose mechanical properties are influenced by the environment in which it is grown. It is universally acknowledged that, even if the same timber structural grade is employed, wood frame walls may exhibit high uncertainty in their behavior under lateral and vertical loads. For instance, previous research [8] has reported variability of about 20% in strength and stiffness for wood frame walls analyzed under similar conditions. Therefore, this section aimed at experimentally analyzing the suitability of Chilean timber products for use in mid-rise buildings, testing the elements that make up a wood frame wall, and verifying the response of walls with different properties under large lateral displacements as those expected during severe earthquakes. Furthermore, it provided relevant data to calibrate and validate the numerical models presented in Section 2.2.

A combination of timber and steel elements make up a wood frame wall. For mid-rise buildings, a typical wall consists of a timber frame (>1200 mm in length) assembled with 35 × 138 mm studs. To resist the high vertical loads, end studs have several members, while interior studs are single members spaced at 400 mm on center. Top and bottom plates consist of double members, and the wall is attached to the floor by means of a steel anchorage system (a discrete or continuous hold down). The lateral capacity of the wall is provided by 9.5–15.1 mm thick sheathing OSB panels on one or both sides of the wall, which are attached to the timber frame with steel nails spaced at 50 to 100 mm on center along the panel edges. At the interior studs, nails are spaced at 200 mm. A schematic configuration of a typical wood frame wall is shown in Fig. 2.

At the first stage of the testing program, forty-five timber studs were mechanically tested under axial load at the Structural Laboratory of the INFOR Institute, in Concepción, Chile, following the guidelines of the Chilean standard NCh3028/1 [10]. Specimens consisted of mechanically graded Chilean MGP10 radiate pine with a cross-section of 35 × 138 mm and 2400 mm long. Additionally, twenty 11.1 mm thick OSB panels (127 × 127 mm) were tested according to the ASTM D2719 standard [11] at the facilities of the APA Engineered Wood Association, in Tacoma, USA, to study their shear capacity in two ortogonal directions. Test results were consistent with those reported by previous investigations [12–15], showing that Chilean wood products meet the requirements for use in structural engineering. Further details of the testing program and experimental results can be found in [16].

Subsequently, thirty-six sheathing-to-framing (S2F) connections were tested at the facilities of the University of Bío-Bío, in Concepción, Chile. The specimens consisted of pneumatically-driven shear OSB-stud joints, employing 70 mm long spiral nails with 3 mm in diameter. The studs were 35 × 138 mm, and the panel thickness ranged from 9.5 to 15.1 mm. Six tests were monotonic and thirty were cyclic, applying the CUREe-Caltech loading protocol proposed by Krawinkler et al. [17]. Results were consistent with previous investigations [12,18–20] in

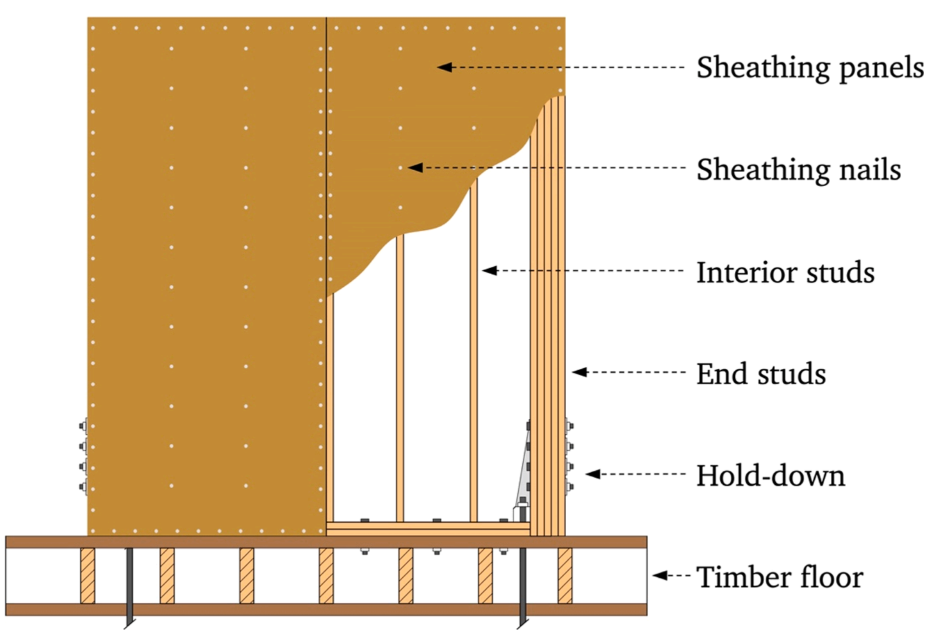

Fig. 2. Schematic configuration of wood frame walls for mid-rise timber buildings.

terms of strength, stiffness, ductility, nonlinear response, and energy dissipation, showing a pinched hysteresis under large reversed displacements. Typical failure modes were observed during the tests: yielding and shear fatigue of nails, nails withdrawal, pulling through of nail heads, and crushing of the OSB panel. A comprehensive report of the results can be found in [21]. The test setup and results for a cyclic specimen are shown in Fig. 3(a) and 3(b), respectively.

Finally, 23 full-scale wood frame walls were tested at the facilities of the Structural Engineering Laboratory at the Pontifical Catholic University of Chile. Seven specimens were tested monotonically and sixteen were tested cyclically applying the CUREe-Caltech protocol [17]. The walls were 2440 mm high and the lengths ranged from 700 to 3660 mm. All specimens were sheathed with 11.1 mm thick OSB panel on both sides, employing 70 mm long spiral nails (3 mm in diameter) spaced at 50 or 100 mm. Two different anchorage systems were used: discrete and continuous hold-downs. The difference between these two anchorage systems is that discrete hold-downs fix the bottom of each wall to the underlying timber floor, while the second consists of continuous steel rods across the wall that transfer high tensile forces through several stories to the foundation. Additionally, Ø1-1/4 × 10″ shear bolts were installed through the bottom plate to prevent sliding of the wall. Results showed a good behavior of the walls under large lateral deformation, having a ductile failure mode after the force peak was reached. The damage was mainly concentrated in the S2F connections located at the central studs and wall corners, with minor damage to the framing and anchorage system. Stiffness and capacity were found to depend on the wall length and nail spacing. Interestingly, it was found that the shear capacity computed by the Special Design Provisions for Wind and Seismic (SDPWS) standard [22] underestimates the strength and overestimated the stiffness for wood frame walls with spiral nails. A detailed report and discussion of the tests and results can be found in [8,23]. The test setup and results for a 2440 mm long wall are shown in Fig. 3(c) and 3(d), respectively.

2.2. Nonlinear modeling

Numerical models are convenient tools to expand the scope of the research beyond the testing laboratory. They provide a means to overcome the physical and economic limitations of the experimental programs, allowing a wider range of scenarios and conditions to be

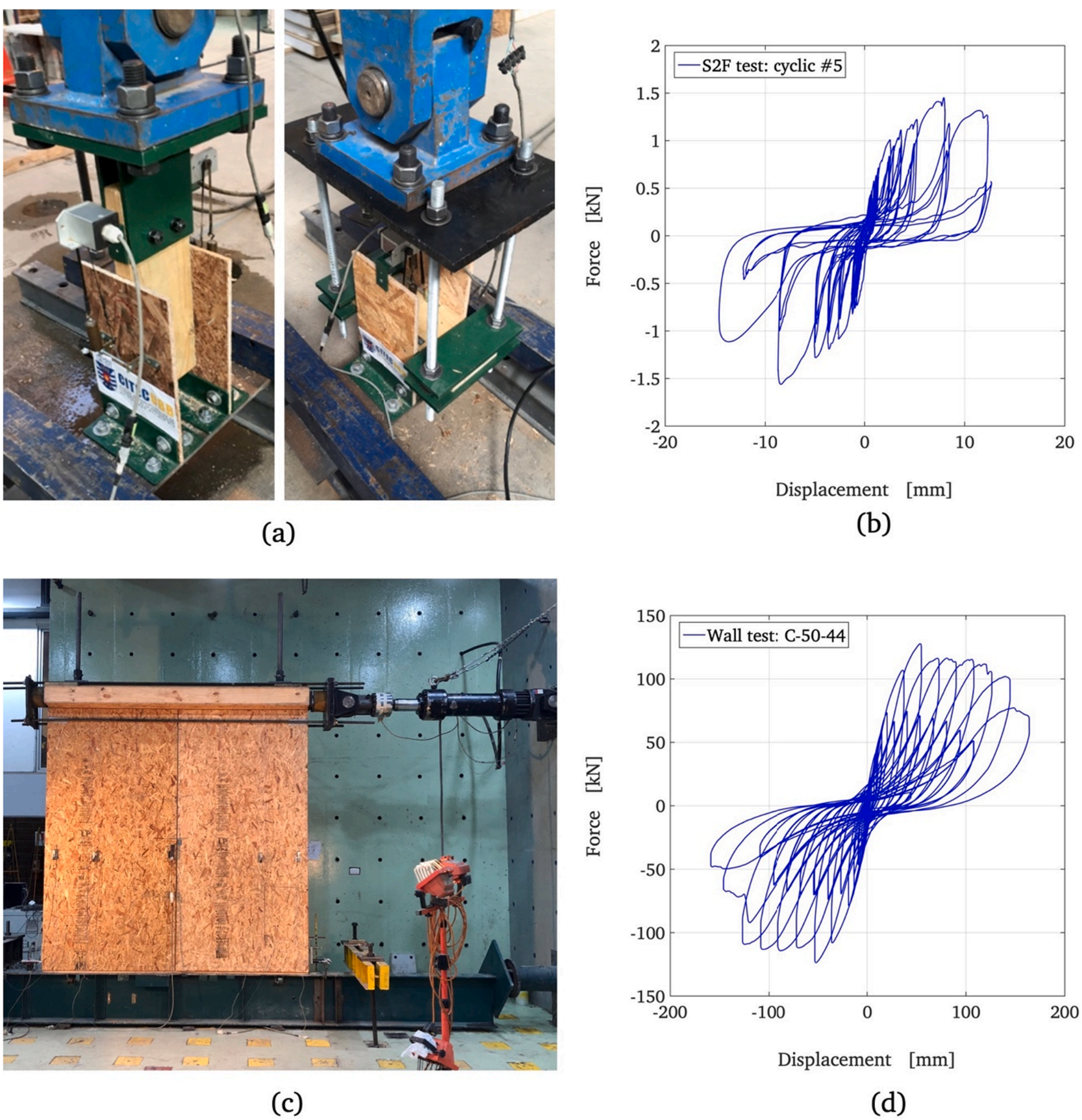

Fig. 3. Experimental program: (a) setup for sheathing-to-framing S2F tests, (b) results of cyclic S2F test #5, (c) setup for full-scale wood frame wall tests, and (d) cyclic results for a 2440 mm long wall with continuous rod hold-downs.

analyzed. Therefore, based on the experimental data discussed in the previous section and the work conducted by previous researchers [12,24], a new modeling approach was developed for the wood frame walls under study. This new model takes into account the special features of the walls for mid-rise buildings [8,25] as presented in Section 2.1 and Fig. 2, allowing accurate nonlinear analyses for large displacements to be conducted.

In order to minimize the computational overheads and the input parameters, the proposed model followed a simplified strategy between mechanistic lumped approaches and complex FEM models. Consequently, the nonlinearity of the model was introduced by the sheathing-to-framing connections employing two uncoupled orthogonal springs with nonlinear behavior under cyclic reversed loads. The remaining wall components were assumed to behave within the elastic regime, employing frame elements for the timber studs, rectangular shear elements for the OSB panels, and linear unidirectional springs for the anchorage system. Fig. 4(a) shows a comparison of the test results and model predictions for a 2440 mm long wall with discrete hold-downs, and Fig. 4(b) pictures a schematic representation of the model and its components. A full description of the modeling approach and its validation with experimental tests can be found in [26].

When developing numerical models for wood frame buildings with several stories and structural elements, an efficient approach is necessary to carry out static and dynamic nonlinear analyses without compromising the available computational resources. Such an approach should capture the intrinsic properties of the nonlinear behavior of timber structures and, at the same time, be efficient enough to maximize the cost-effectiveness of the analyses. For wood frame buildings, Pei and van de Lindt [27] proposed a simple approach that employed springs and rigid diaphragms to model the 3D behavior of the structure under lateral loads, whose accuracy has been validated with full-scale tests of low- and mid-rise assemblies [28,29]. As illustrated in Fig. 5, such a model uses a nonlinear horizontal spring to represent the shear response of each wall, and bi-linear vertical springs to capture the wall uplifting due to the anchorage elongation. The horizontal spring employs the MSTEW nonlinear hysterical model proposed by Folz and Filiatrault [12], which is able to capture phenomena such as strength degradation, stiffness degradation, and pinching, commonly observed for wood frame walls under large lateral deformations. The horizontal floor diaphragm in each story is modeled as a rigid body (i.e., a rigid plate) with 6-DOF at its center of gravity, where the seismic mass of the floor is concentrated. A detailed formulation of the model can be found in [27].

Employing the modeling approach shown in Fig. 4(a) and the shear data from the experimental program, the parameters of the MSTEW model were calibrated for wood frame walls with different properties. This way, a database was generated with the aim of providing a robust framework to develop simplified nonlinear models for wood frame structures. These results can be found in [30]. By way of example, Fig. 6 shows a comparison between the shear response of a 2440 mm long wall test and the predictions of the MSTEW model. As can be noted from the plots, with a very low computational effort, the MSTEW model accurately predicts the test results even for large deformations, properly capturing the nonlinear behavior of the specimen in terms of strength, stiffness, and deformation capacity. This simplified modeling approach will be used in subsequent sections to study the seismic behavior of multistory wood frame buildings and validate the new set of SPFs.

2.3. Architectural archetypes

The validation of a set of SPFs through the FEMA P-695 guidelines [1] requires analyzing the seismic behavior of a comprehensive group of buildings (structural archetypes) in order to determine if the new SPFs lead to structures that reach appropriate performance levels. Such a group of structural archetypes must cover a thorough spectrum of scenarios regarding architecture, structural configuration, seismic design load, and structure emplacement. In this section, the different architectural archetypes employed in this research are briefly presented and discussed. After a comprehensive analysis of the most common floor-plan configurations in the Chilean real estate market of concrete and masonry buildings, four architectures (so-called “Q”, “C”, “P”, and “D”) were developed for this investigation. As Fig. 7 shows, the floor-plans take into account the inherent features of wood frame buildings regarding space distribution, placement of structural elements, and climatization needs, and embrace different architectural possibilities for both the private and social housing markets. A detailed report on the floor-plans development can be found in [31].

The floor area of the archetypes ranged from 252 to 530 m^2, with a space efficiency η_a above 93% in all cases. The floor-plans Q and P were mostly square-shaped with a plan aspect ratio equal to 1.50 and 1.38, while for the plans C and D, the plan aspect ratio was 2.05 and 3.6, respectively. Considering only structural walls (wall aspect ratio ≤ 2) in each floor-plan, the wall density for a given direction (X or Y) ranged from 3.05% to 5.96%, a value consistent with previous investigations [7], and somewhat higher than that of other materials. For instance, for

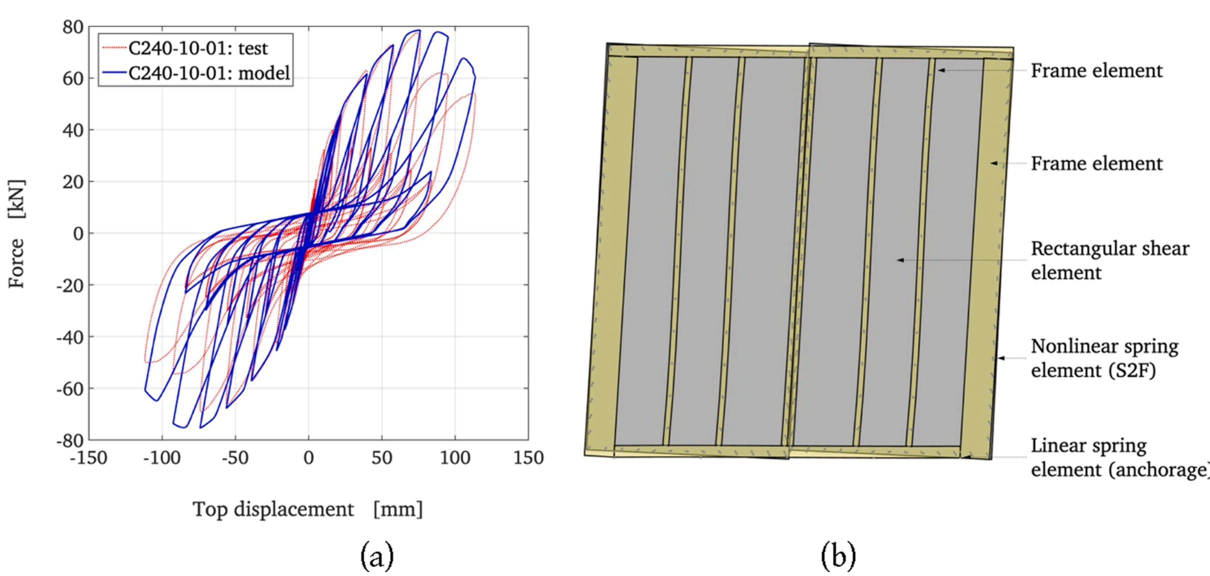

Fig. 4. (a) Comparison between test results and model predictions for a 2440 mm long wall with discrete hold-downs, and (b) schematic representation of the proposed modeling approach.

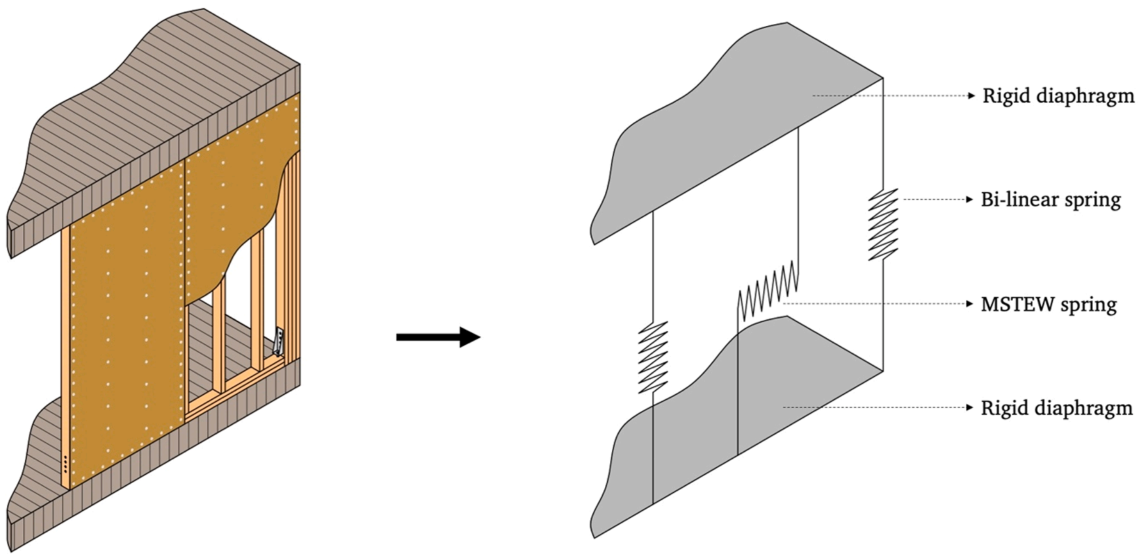

Fig. 5. Simplified modeling approach proposed by Pei and van de Lindt [27] for wood frame structures.

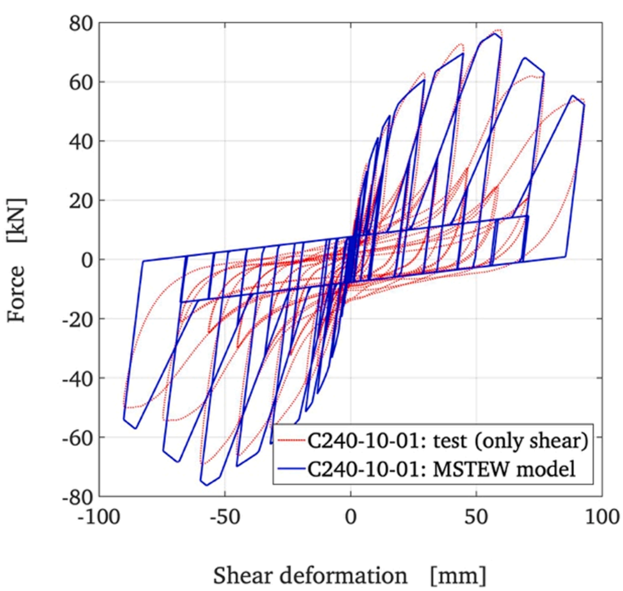

Fig. 6. Comparison between shear test results and MSTEW model predictions for a 2440 mm long wall with discrete hold-downs.

Chilean concrete buildings, the typical wall density is about 2.8% [32]. The average ratio of wall linear meters (X or Y) to the floor perimeter was 1.11. Detailed information on the architectural archetypes is listed in Table 1.

2.4. Structural archetypes

In addition to the architectural floor-plans discussed in the previous section, different design scenarios were taken into account when developing the structural archetypes for this investigation. Firstly, following the Chilean NCh433 standard [3], two seismic zones (Z1 and Z3) and four soil classes (from A to D) were considered when siting the archetypes. This resulted in different design base shear values since the design spectrum of the NCh433 standard [3] is a function of the seismic zone and soil class. Secondly, two SPF sets were included when designing the archetypes: (1) R = 5.5 & $\Delta_{max} = 0.002$, and (2) R = 6.5 & $\Delta_{max} = 0.004$. The first set aimed at validating the suitability of the current regulations in the NCh433 standard [3], while the second set proposes new less-restrictive SPFs for wood frame buildings. The values for the second set were selected after a preliminary parametric study on selected archetypes to find the SPFs that maximize the cost-benefit ratio of the structural design. Thirdly, the height of the buildings ranged from three to six stories, covering the most common applications for wood frame mid-rise structures in Chile and providing a wide range of fundamental periods T_1 in the archetype set (from 0.27 s to 1.01 s). And fourthly, two solutions were implemented regarding the structural anchorage system: (1) discrete hold-downs, and (2) continuous rod hold-downs. This way, variations on the strength and stiffness of the walls due to the anchorages were considered when analyzing the archetypes. After permuting the variables listed above along with the architectural floor-plans described in Section 2.3, a set of 201 structural archetypes was obtained for this investigation. A detailed report of the set can be found in [33]. Table 2 summarizes the design scenarios and building features of the archetype set.

Structural designs were carried out for each archetype in the set according to the different design scenarios and building features listed in Table 2. Design loads were computed from the NCh433 guidelines [3]. A live load L equal to 200 kg/m^2 for residential buildings was considered in all archetypes, and dead loads D were calculated for each case based on the self-weight of structural elements and timber slabs (dead loads ranged from 200 to 250 kg/m^2, approximately). Subsequently, the seismic mass of each floor was calculated as D + 0.25L [3]. As established by the NCh433 standard [3], for archetypes up to 5 stories the seismic design loads were obtained through static analyses on linear models of the archetypes, while the 6-story archetypes employed a modal analysis to compute the design loads. The design base shear was calculated from code-defined acceleration spectra as a function of the seismic zone, soil type, occupancy category, and R factor. An occupancy category II was considered for all archetypes. It should be noted that for all 6-story archetypes an R_o factor equal to 7.0 was considered, since the NCh433 standard [3] establishes this criterium when modal analyses are used. Therefore, for these archetypes the sets of SPFs were: (1) $R_o = 7.0$ & $\Delta_{max} = 0.002$, and (2) $R_o = 7.0$ & $\Delta_{max} = 0.004$. When calculating the base shears through static analyses, the fundamental period of the structure was computed using Equation (1) proposed by [34]:

$$T_1 = 2\pi\sqrt{\frac{2\delta_n}{3g}} \quad (1)$$

where δ_n is the roof displacement of the structure when a lateral load equal to the seismic weight of the building is applied on a linear model.

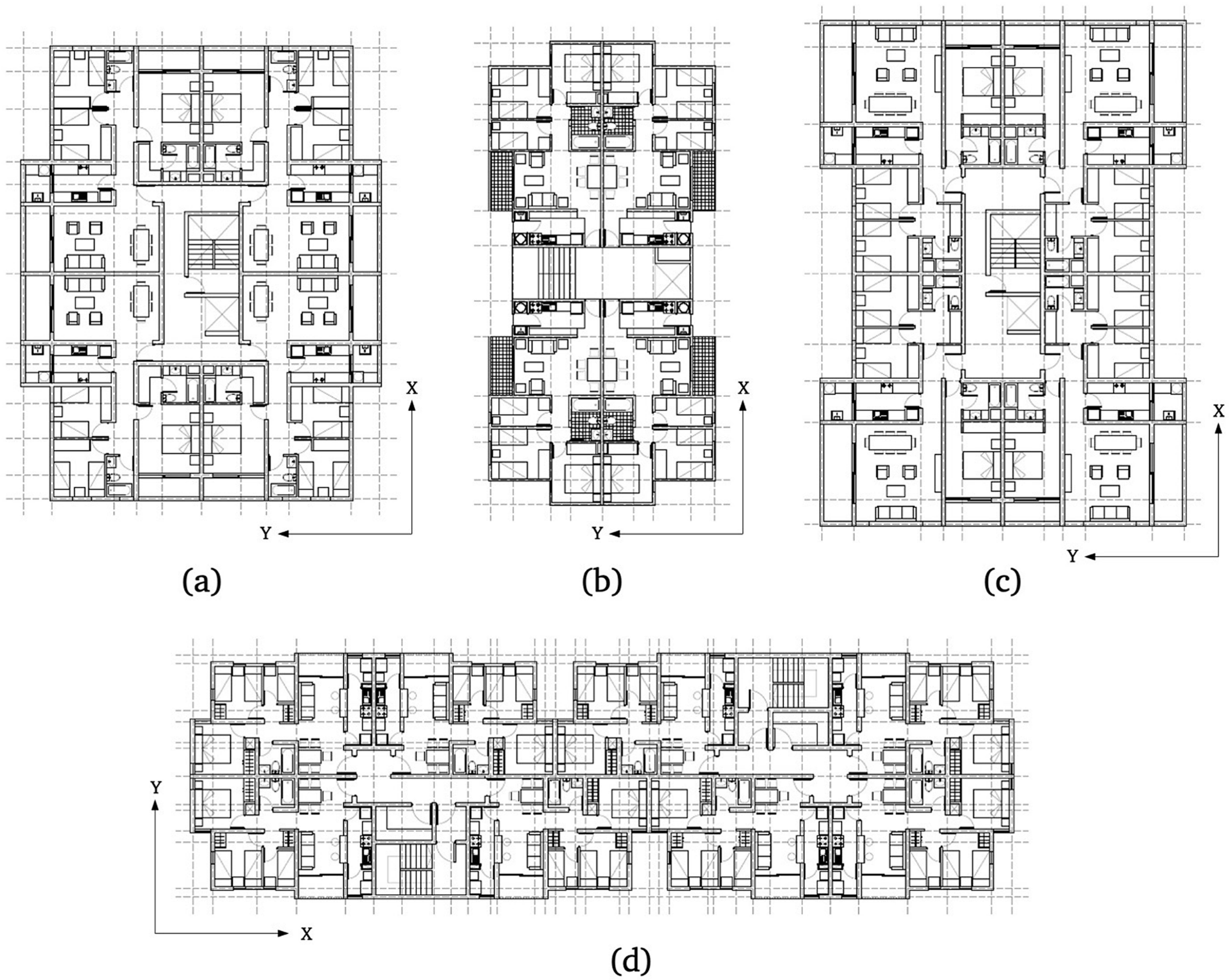

Fig. 7. Floor-plan configurations developed for this investigation: (a) floor-plan “Q”, (b) floor-plan “C”, (c) floor-plan “P”, and (d) floor-plan “D”.

Table 1
Geometric parameters of the architectural archetypes: B_x and B_y = plan dimensions, B_x/B_y = plan aspect ratio, A = floor area, A_c = core area (elevators and staircases), η_a = space efficiency = 1-(A_c/A), ρ_x and ρ_y = wall density, P = perimeter, L_x and L_y = wall linear meters, L_x/P and L_y/P = ratio of wall linear meters to perimeter.

Archetype	B_x [m]	B_y [m]	B_x/B_y	A [m^2]	A_c [m^2]	η_a [%]	ρ_x	ρ_y	P [m]	L_x [m]	L_y [m]	L_x/P	L_y/P
Q	24.23	16.16	1.50	436.61	17.07	96.09	3.69	3.73	86.9	101.30	102.32	1.17	1.01
C	24.75	12.09	2.05	252.66	14.98	94.07	3.10	5.96	78.58	49.24	94.61	0.63	1.92
P	26.92	19.54	1.38	491.88	17.07	96.53	3.63	3.05	99.8	112.26	94.36	1.12	0.84
D	43.89	12.20	3.60	530.28	32.58	93.86	3.84	4.61	128.05	127.86	153.64	1.00	1.20

Table 2
Design scenarios and building features considered in the structural archetype set.

Variable	Variations
Floor-plan	Q, C, P, and D
Seismic zone	Zone 1 and Zone 3
Soil class	A, B, C, and D
SPF sets	0.002 h & 5.5 and 0.004 h & 6.5 (R_o = 7.0 for 6-story buildings)
Number of stories	3, 4, 5, and 6
Anchorage system	Discrete and continuous hold-down
Total archetypes	**201**

Additionally, accidental torsion effects were also considered when calculating the design base shear, incorporated as a geometric eccentricity in the structural design [3]. In the static analyses, the vertical distribution of the shear loads for each floor followed the guidelines in Section 6.2.5 of the NCh433 standard [3]. The shear load for each wall of the floor was distributed assuming a rigid diaphragm behavior of the timber slab. As previous researchers have reported, this is a suitable assumption when the floor-plan is regular, a properly detailing is used, and the floor/wall stiffness ratio does not exceed nominal values as defined by [35,36]. Thereby, the shear load for each wall was computed proportionally to its stiffness. Regarding the vertical loads on the wall, they were calculated based on the tributary areas determined from the floor-plan distribution for each wall. Finally, the design properties of walls (strength and stiffness) were estimated from the SDPWS guidelines [22] for elements with smooth shank nails, the mechanical characteristics of materials from the Chilean NCh1198 standard [15], and the capacities of the hold-down devices (discrete and continuous) from the design catalogs provided by the supplier [37,38]. A thorough report of the structural design process can be found in [39].

2.5. Ground motion selection

When evaluating the seismic behavior of structural archetypes with the aim of validating a new set of SPFs, the FEMA P-695 guidelines [1] require performing nonlinear static and dynamic analyses using a numerical model of each archetype. Regarding dynamic analyses, these are carried out in the form of an incremental dynamic analysis (IDA) for each archetype of the set. An IDA is a series of response-history nonlinear analyses employing a pre-defined group of ground motions, whose amplitude increases progressively until a given performance level is reached [40]. In this context, the FEMA P-695 standard [1] provides two ground motion sets to be used in the IDAs. The first set consists of 22 pairs of far-field accelerograms recorded at sites more than 10 km away from the fault rupture, and the second set of 28 pairs of near-field accelerograms recorded at sites less than 10 km away from the fault rupture. Both the far-field and near-field accelerograms were recorded from shallow crustal earthquakes (typical in the Western United States), and they do not include records from deep subduction earthquakes such as those expected in Japan, New Zealand, or in areas on the Pacific Coast in South America. This limits the application of the sets provided by the FEMA P-695 methodology in regions threatened by subduction earthquakes since the intrinsic features of subduction records (such as frequency content, record duration, or energy released) are neglected, leading to obtaining non-conservative results from the IDAs [41]. Therefore, since Chile is located in a seismic subduction area, a new set of ground motions that is entirely consistent with the FEMA P-695 guidelines and properly includes subduction ground motions was developed for this research.

The new ground motion set consisted of 26 pairs of accelerograms (horizontal components) obtained from seismological reports of different countries around the globe. In order to avoid bias towards a particular region, records were chosen regardless of the zone or country of origin. The ground motions were selected such that 2/3 were subduction records and 1/3 crustal ones. Therefore, the set was comprised of 18 records from subduction earthquakes and 8 from shallow crustal earthquakes, of which 3 were from thrust faults and 5 from strike-slip faults. Earthquake magnitudes ranged from M = 6.5 to 9.0 Mw, covering seismic events in a time window of 30 years, approximately. Fig. 8 shows the response spectra for the 26 pairs of records and the mean spectrum of the set plus one and two standard deviations. It can be observed that the average spectral acceleration for short periods is close to 0.8 g, and for a 1-second period, it is about 0.35 g. The transition from the constant spectral acceleration zone to the constant velocity zone occurs at T = 0.5 s, a value consistent with the expected response of soft rock sites or rigid soils. A complete report of the ground motion set, selection criteria, normalization procedure, spectral shape factors, and further analyses can be found in [41].

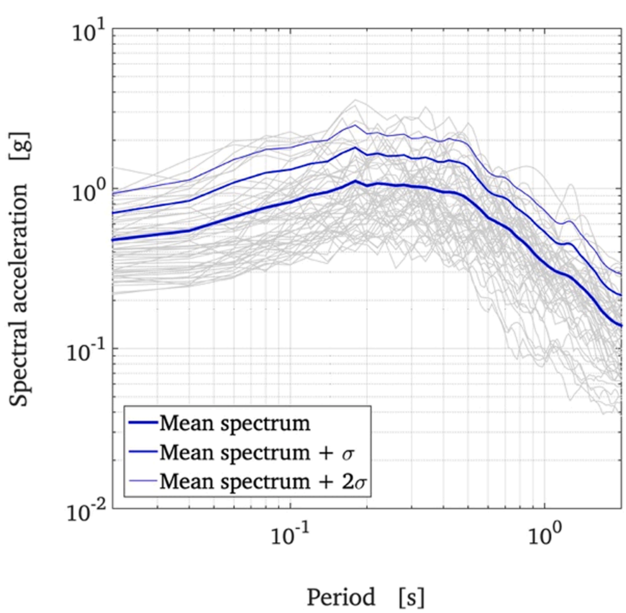

Fig. 8. Response spectra of the 26 pairs of records and mean spectrum of the set plus one and two standard deviations.

2.6. Nonlinear static and dynamic analyses

This section briefly summarizes the nonlinear static and dynamic analyses conducted on each structural archetype of Section 2.4. As prescribed by the FEMA P-695 guidelines [1], these analyses provided a means for a rational and sound validation of the new set of SPFs as will be discussed later in this paper. Firstly, employing the simplified modeling approach presented in Section 2.2, a nonlinear model was developed for each of the 201 structural archetypes of the set employing the SAPWOOD [42] software. Static analyses were conducted on each model in the X and Y direction employing a modal adaptive lateral load distribution over the building height. This way, valuable information was obtained for each archetype, such as the system over-strength, overall stiffness, ductility, damage distribution, among others. By way of example, Fig. 9(a) shows the base-shear versus roof-displacement plot for archetype 103, i.e., a 5-story building, floor-plan “P”, seismic zone A, soil type A, SPFs 6.5 & 0.004, and discrete hold-downs. A full report of the static results for all archetypes can be found in [33].

Dynamic analyses consisted of a bidirectional IDA for each archetype employing the ground motion set presented in Section 2.5. Each record pair of the set was applied twice to each model, once with the components oriented along the principal directions, and then again with the components rotated 90 degrees. The records were systematically scaled based on the spectral acceleration $Sa(T_1)$ corresponding to the fundamental period of the building, increasing the record intensity until structural collapse took place defined as the occurrence of a 3% interstory drift at any floor. Subsequently, the collapse margin ratio was computed as $CMR = S_{CT}/S_{MT}$, where S_{CT} is the mean collapse capacity defined as the mean spectral acceleration from the IDA curves for a 3% drift, and S_{MT} is the code-defined spectral acceleration corresponding to the maximum considered earthquake MCE for the building under analyses [3,43]. Fig. 9(b) shows the IDA results for archetype 103 along with the S_{CT}, S_{MT}, and CMR values. Dynamic analyses considered a damping ratio equal to 1%. P-delta effects were not considered.

According to the FEMA P-695 guidelines [1], the validation of a new set of SPFs is carried out by means of the adjusted collapse margin ratios ACMR of the structural archetypes. ACMRs are computed as $ACMR = CMR \times SSF \times 1.2$, where SSF is the spectral shape factor to take into account the spectral shape of the ground motions employed in the dynamic analyses [1,41], and 1.2 is a factor to account for the 3D dynamic analysis effects induced by the numerical models [1]. The SSF value is a function of the ductility and fundamental period of the archetype under study and is specific for the ground motion set used in the analysis. A detailed report of the SSFs employed in this research can be found in [41]. For the example shown in Fig. 9(b), $ACMR = 3.04 \times 1.26 \times 1.2 = 4.59$.

3. Results and discussion

3.1. Validation of seismic performance factors through ACMRs

The suitability of a new set of SPFs is assessed through evaluating the acceptability of the adjusted collapse margin ratios ACMR calculated

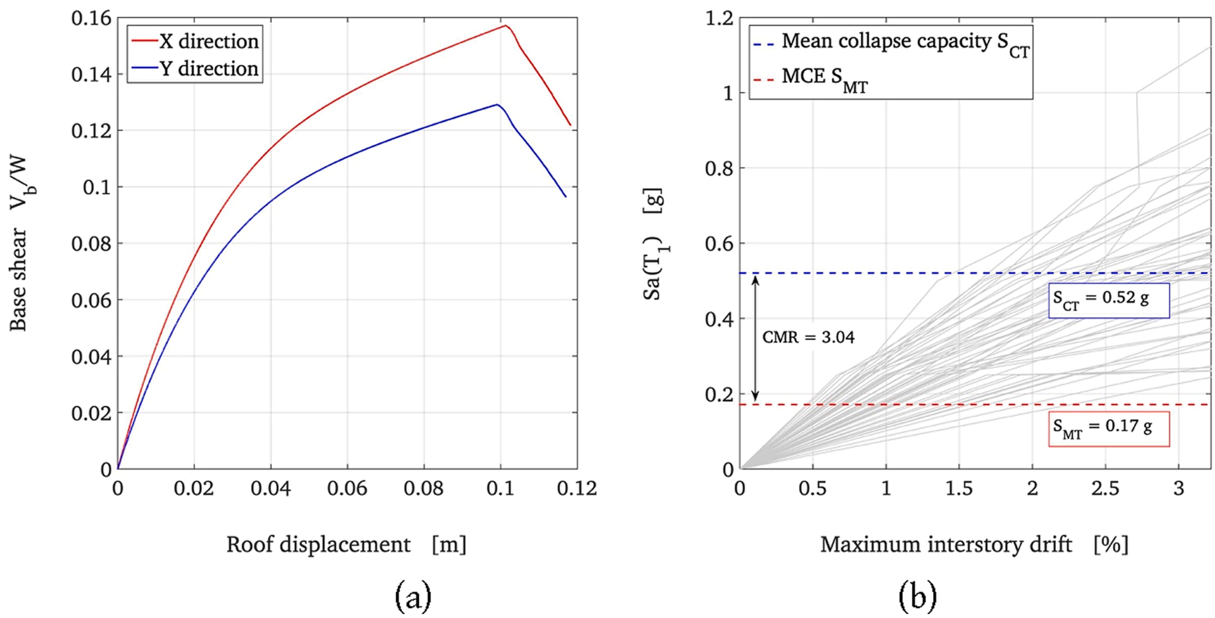

Fig. 9. Nonlinear numerical results for archetype 103: (a) static lateral results for the X and Y directions, and (b) IDA results along with the mean collapse capacity S_{CT}, MCE spectral acceleration S_{MT}, and collapse margin ratio CMR.

from the incremental dynamic analyses, as detailed in Section 2.6. Such acceptability is determined by comparing the calculated ACMRs to minimum acceptable values $ACMR_{min}$ that guarantee to meet a given collapse probability for the structural archetype under study. The benchmark $ACMR_{min}$ values depend on two factors: (1) the quality of the information employed in the process, and (2) the limits established for the structural collapse probability.

The quality of the information and data employed over the course of the investigation has a direct influence on the total uncertainty of the results. Therefore, the higher the total uncertainty of the process, the higher the ACMR values must be in order to meet the acceptable collapse probabilities set for the structural archetypes. Four uncertainty sources [1] have been considered in this research: (1) record-to-record variability β_{RTR}, due to uncertainty in the response of the structural archetypes to different ground motions, (2) design requirements variability β_{DR}, related to the completeness and robustness of the design guidelines employed when developing the structural archetypes, (3) test data variability β_{TD}, related to the robustness of the experimental information used to define the system and develop the numerical models, and (4) modeling variability β_{MDL}, related to how well the numerical models reproduce the full range of structural responses and capture collapse behavior by means of direct simulated or non-simulated element checks. Following the guidelines of the FEMA P-695 methodology [1], the variability values for this research were defined as $\beta_{RTR} = 0.4$, $\beta_{DR} = 0.1$, $\beta_{TD} = 0.1$, and $\beta_{MDL} = 0.2$. The total variability β_{TOT}, computed as the squared root of the summation of the squares of the individual variabilities, was equal to $\beta_{TOT} = 0.469$. A full description of this process can be found in [1].

The fundamental aspect when evaluating the suitability of a set of SPFs is that an acceptably low, yet reasonable, probability of collapse can be reached by the structural archetypes designed with such SPFs. In this context, the guidelines of the FEMA P-695 methodology [1] recommend assessing the collapse probabilities at two different levels: individual and group. At the individual level, each structural archetype is recommended to meet a collapse probability equal to 20% for MCE ground motions. For the group level evaluation, firstly, the archetypes are binned into performance groups that reflect their primary differences in configuration and structural design, providing a basis for statistical assessment of the SPFs sets under investigation. In this research, five aspects were considered when identifying the performance groups: (1) the SPFs used for design, (2) anchorage system, (3) seismic zone, (4) soil type, and (5) fundamental period of the archetype. Fundamental periods were classified into two categories: short and long ones, defined by the boundary between the constant spectral acceleration and constant velocity regions of the design spectrum. Since the design spectra of the NCh433 standard [3] are defined as continuous functions and not as piecewise-linear functions (for instance, as Newmark-Hall spectra), the boundary between the constant spectral acceleration and constant velocity regions was defined following the recommendations by the ASCE 7–16 standard [4] to define a transition period. Taking into account the five binning aspects described above, 33 performance groups were identified for this research out of the 201 structural archetypes presented in Section 2.4. Further details about the development of the performance groups can be found in [44]. Finally, as suggested by the FEMA P-695 guidelines [1], to validate the suitability of the SPFs set used for structural design, each performance group should meet an average collapse probability equal to 10% for MCE ground motions. It can be noted that the collapse probability for performance groups is limited to one -half of that one for individual archetypes. This judgment aims at recognizing the variability in the seismic response of the structural systems, providing a criterion to assess the acceptability of potential outliers within each performance group.

In order to evaluate the suitability of the SPF sets, the benchmark $ACMR_{min}$ values are defined based on the total variability β_{TOT} and the collapse probability limits established for both individual archetypes and performance groups. $ACMR_{min}$ values are computed assuming that the distribution of the spectral intensities at collapse level is lognormal with a median value S_{CT} and a lognormal standard deviation equal to the total variability β_{TOT}. Considering $\beta_{TOT} = 0.469$, the $ACMR_{min}$ values for a 20% and 10% collapse probability are $ACMR_{20\%} = 1.49$ and $ACMR_{10\%} = 1.84$, respectively [1]. Fig. 10(a) shows the ACMR values for the 201 structural archetypes analyzed in this research along with the $ACMR_{20\%}$ limit, and Fig. 10(b) shows the average ACMR values for the 33 performance groups along with the $ACMR_{10\%}$ limit. The results were classified by the SPFs set used for structural design: $R = 5.5$ & $\Delta_{max} = 0.002$, and $R = 6.5$ & $\Delta_{max} = 0.004$. It should be highlighted that the SPFs for six-story buildings were $R = 7.0$ & $\Delta_{max} = 0.002$ and $R = 7.0$ & $\Delta_{max} = 0.004$, respectively.

Results in Fig. 10(a) show that the 201 structural archetypes analyzed in this research meet the minimum ACMR requirement to

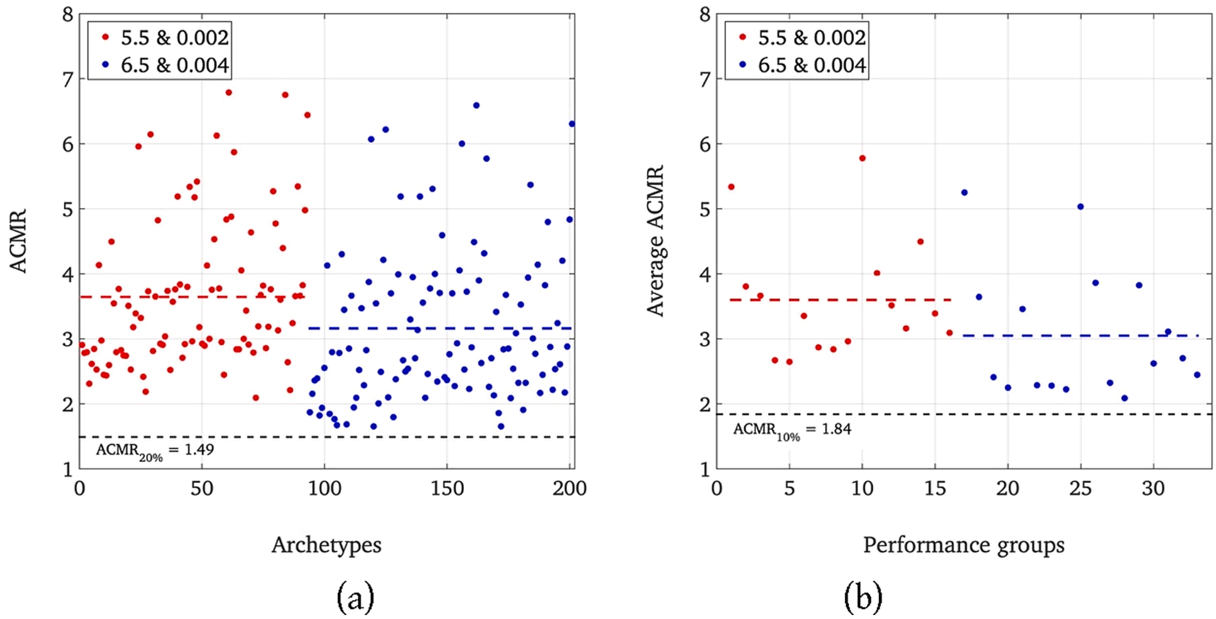

Fig. 10. ACMR results and $ACMR_{min}$ values for: (a) individual structural archetypes, and (b) performance groups. Six-story buildings employed R = 7.0 & Δ_{max} = 0.002 and R = 7.0 & Δ_{max} = 0.004, respectively.

reach a 20% collapse probability limit. The average ACMR for each set of SPFs is 3.64 and 3.16, respectively, with standard deviations equal to 1.12 and 1.17. When the SPFs changed from R = 5.5 & Δ_{max} = 0.002 to R = 6.5 & Δ_{max} = 0.004, the average ACMR reduced by 13.3%, however, no archetype went below the $ACMR_{20\%}$ requirement. This means that, even though the new set of SPFs results in less conservative structural systems, they still have an acceptable low probability of collapse that does not compromise the structural performance or lead to life-threatening scenarios. On the other hand, results in Fig. 10(b) show that all performance groups are above the $AMCR_{10\%}$ limit, with average values of 3.60 and 3.05 for each SPF set, and standard deviations equal to 0.92 and 0.99, respectively. The average ACMR value reduced by 15.3% when the new SPF set was employed; however, no performance group showed an average ACMR lower than the 10% collapse probability limit. This way, the 201 archetypes analyzed in this research prove to meet the FEMA P-695 requirements [1] at the individual and group check level, showing that the new proposed set of SPFs results in code-compliant structures with an improved cost-effectiveness ratio. For instance, a brief analysis of a 5-story building showed that changing the SPFs from R = 5.5 & Δ_{max} = 0.002 to R = 6.5 & Δ_{max} = 0.004 during the design phase resulted in a 40.4% saving in nailing, 15.9% in OSB panels, and 7.3% in timber studs.

It is interesting to note that according to Fig. 10 several archetypes have a considerable high ACMR value compared to the minimum required to guarantee structural safety. As Fig. 10(a) shows, out of the 201 archetypes, 35 have an ACMR over three times the $ACMR_{20\%}$ limit (i.e., 3 × 1.49 = 4.47). This means that about 17% of the archetypes resulted in over-conservative structural systems regardless of the SPF set

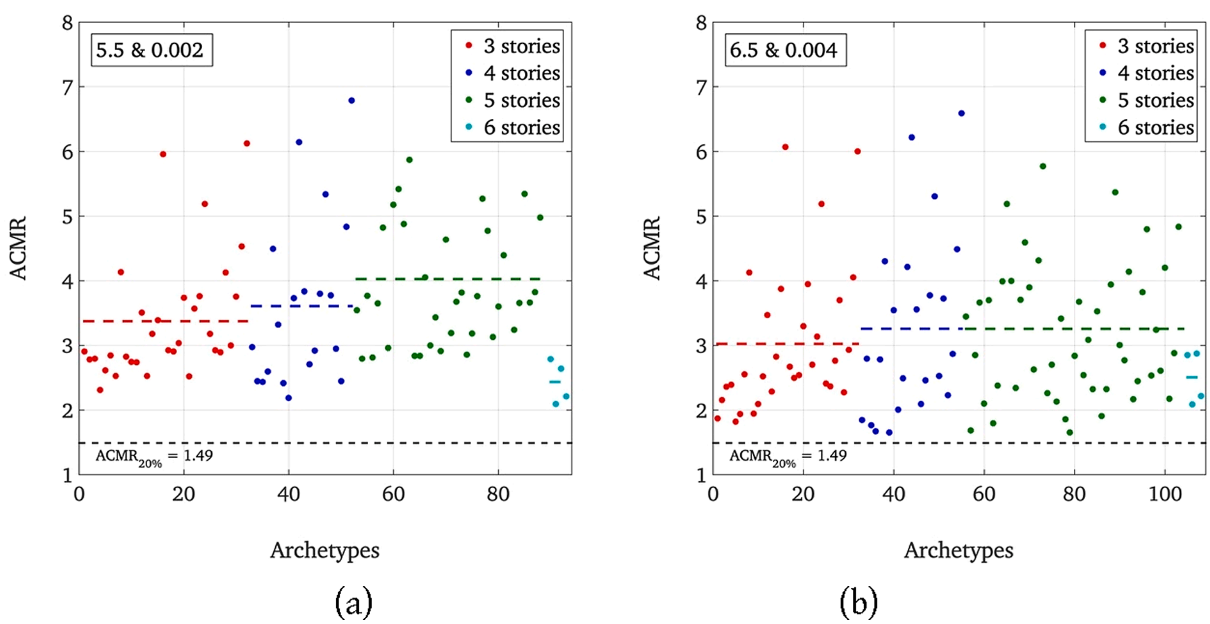

Fig. 11. ACMR results classified by number of stories: (a) archetypes designed with R = 5.5 & Δ_{max} = 0.002, and (b) archetypes designed with R = 6.5 & Δ_{max} = 0.004. Six-story buildings employed R = 7.0 & Δ_{max} = 0.002 and R = 7.0 & Δ_{max} = 0.004, respectively.

employed during design. Seeking to understand this phenomenon, Fig. 11(a) and 11(b) sort out the ACMR results by SPF sets and number of stories, respectively. It can be observed that the building height does not have a significant influence on the lateral behavior of the structure since similar average ACMR values are observed for the different number of stories analyzed. Interestingly, the six-story archetypes for both SPF sets show relatively low ACMRs compared to other building heights. A detailed analysis showed that this phenomenon was not due to the number of stories itself, but to the design procedure employed for these archetypes. As explained in Section 2.4, all 6-story archetypes used an R_o factor equal to 7.0 and their seismic design loads were computed by means of modal analysis, as the NCh433 standard requires [3]. Therefore, it is noted that these two guidelines lead to more efficient structural systems in terms of seismic behavior, since the archetypes designed under such requirements show ACMR values that satisfy the 20% collapse probability requirement and do not exhibit an over-conservative response. Thereby, even though modal analyses might be more time consuming to carry out when compared to static analyses (i.e., because it is necessary to develop a numerical model of the structure), they proved to be an efficient approach to optimize the cost-effectiveness when designing structural systems under seismic loads.

On the other hand, it is of relevant interest to analyze the influence of the design soil class on the ACMR of the archetypes. Fig. 12(a) and 12(b) show the ACMR results classified by SPF sets and soil classes, respectively. Unlike the results shown in Fig. 11, Fig. 12 shows a clear correlation between the soil class and ACMR values: the "better" the soil class, the higher the ACMR. The design soil class has a direct influence on the performance of the structural archetypes since it determines (along with the seismic zone and occupancy category) the design base shear computed from code-defined spectra. Soil quality ranges from A to D, being A a "good" soil and D a "poor" soil, therefore, archetypes on soil A were designed with a lower base shear compared to those on soil D. However, when calculating ACMRs (i.e., $CMR = S_{CT}/S_{MT}$, and $ACMR = CMR \times SSF \times 1.2$), S_{MT} values are also a function of the soil class, thereby, the differences in design base shear should not be reflected in the ACMR results, opposite of what Fig. 12 shows. A careful analysis of the archetypes showed that the trend observed in Fig. 12 is not due to the soil class itself, but to the minimum base shear requirement of the NCh433 standard [3].

When designing any structure under the NCh433 standard [3], the spectrum-computed base shear is required not to be less than a minimum value given by $C_{min} = A_0S/6g$, where A_0 depends on the seismic zone, and S depends on the soil type. A_0 is equal to 0.2 g, 0.3 g, and 0.4 g for seismic zones 1, 2, and 3, and S is equal to 0.9, 1.0, 1.05, and 1.2 for soil classes A, B, C, and D, respectively. After analyzing the ACMR results of the 201 archetypes, it was found that the minimum base shear C_{min} requirement of the NCh433 standard might be somewhat restrictive for soils A, B, and C, leading to conservative results compared to archetypes where the minimum base shear C_{min} did not control the structural design. By way of example, Fig. 13 shows a comparative analysis of the design base shear versus the ACMR parameter for a 5-story building, archetype "C", seismic zone 1, R = 5.5, and $\Delta_{max} = 0.002$. Soil classes A, B, C, and D were analyzed, and the minimum base shear requirement C_{min} for each soil class is shown by vertical dashed lines. For the soil

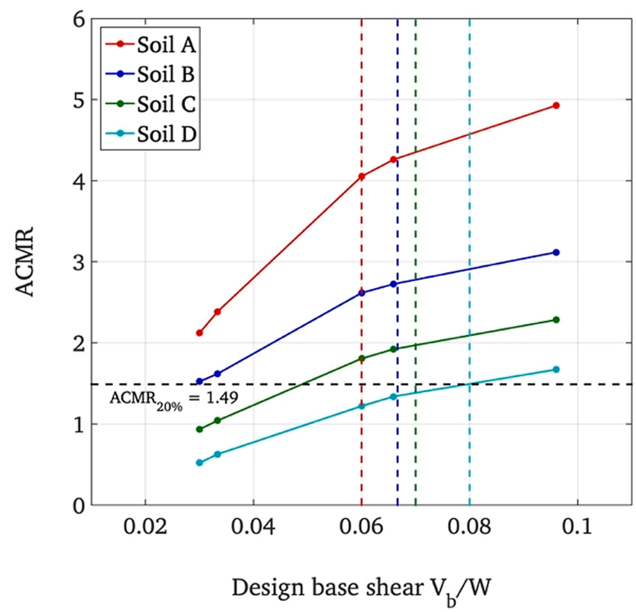

Fig. 13. Comparative analysis of design base shear versus the ACMR parameter for a 5-story building, archetype "C", seismic zone 1, R = 5.5, and $\Delta_{max} = 0.002$. The minimum base shear requirement C_{min} for each soil class is shown by the vertical dashed lines.

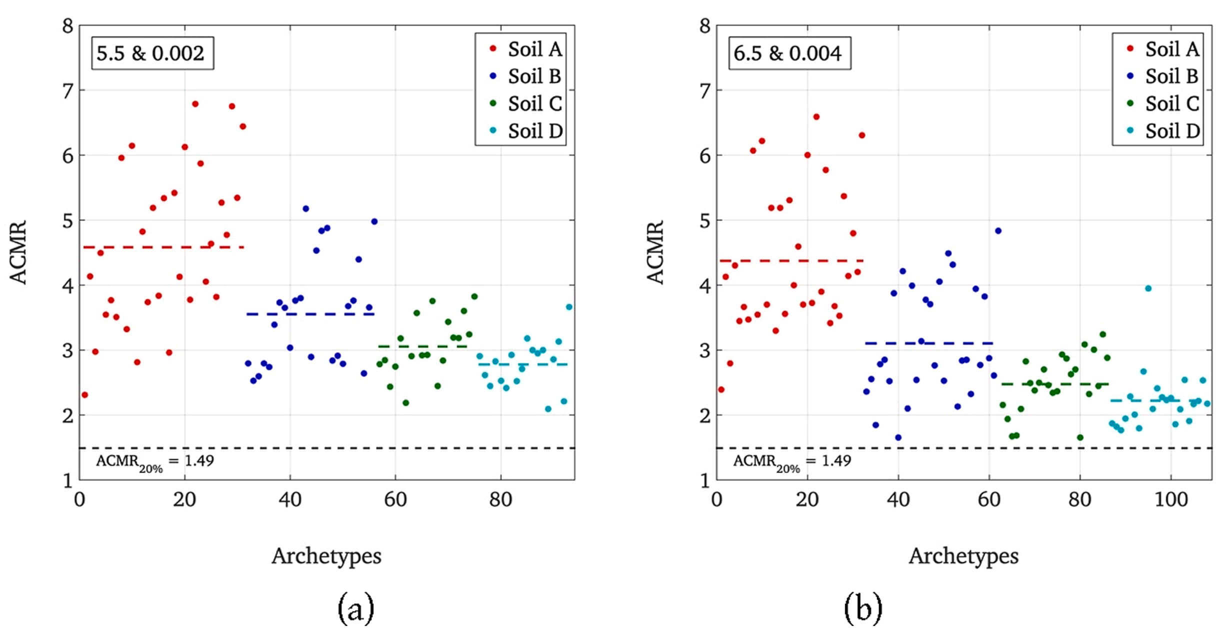

Fig. 12. ACMR results classified by soil class: (a) archetypes designed with R = 5.5 & $\Delta_{max} = 0.002$, and (b) archetypes designed with R = 6.5 & $\Delta_{max} = 0.004$.

class D, it can be observed that the C_{min} value is just right to meet the 20% collapse probability limit. However, for the other soil classes, the C_{min} requirement is much higher than the necessary to meet the 20% limit. This explains the high average ACMR values for soils A, B, and C observed in Fig. 12, since several archetypes were designed under the C_{min} requisite.

To better understand the effect of C_{min} on the ACMRs, Fig. 14 shows the results for the entire set of archetypes analyzed in this study after removing the data for the cases where the structural design was controlled by the C_{min} requirement. For these results, the average ACMRs are 3.14 and 2.45 for each SPF set, with standard deviations equal to 0.64 and 0.55, respectively. By comparing Fig. 14 and Fig. 10 (a), it can be noted that when the C_{min}-controlled archetypes are not considered, the average ACMRs decreased by 13.9% and 22.4%, and the standard deviations decreased by 43.1% and 52.9% for each SPF set, respectively. These findings remark that the C_{min} requirement of the NCh433 standard [3] leads to inflated results regarding collapse ratios, biasing the average data for the entire set. However, it should be highlighted that the conservatism of the C_{min} requirement for "good" soils is due to the inherent uncertainty of the seismic hazard, aiming at providing a design base shear high enough to guarantee the resilience of the structures under moderate and severe earthquakes. Therefore, further research is needed to evaluate the suitability of the C_{min} requirement of the NCh433 standard [3].

3.2. Performance levels other than collapse

As presented in the previous section, the evaluation of the suitability of a given set of SPFs through the FEMA P-695 guidelines is carried out by analyzing collapse probabilities under spectral accelerations equal to the code-defined MCE seismic hazard. This way, an acceptably low probability of life-threatening scenarios can be guaranteed for the structures under study. However, it is also of relevant interest to examine the behavior of the archetypes under seismic demands with a lower return period and higher exceedance probability, and how performance levels other than collapse may threaten the resilience of the structure under such seismic demands. This concept is consistent with the current philosophy of perform-based seismic design PBSD, which seeks that modern structures, besides not collapsing under severe earthquakes, show limited or negligible structural and non-structural

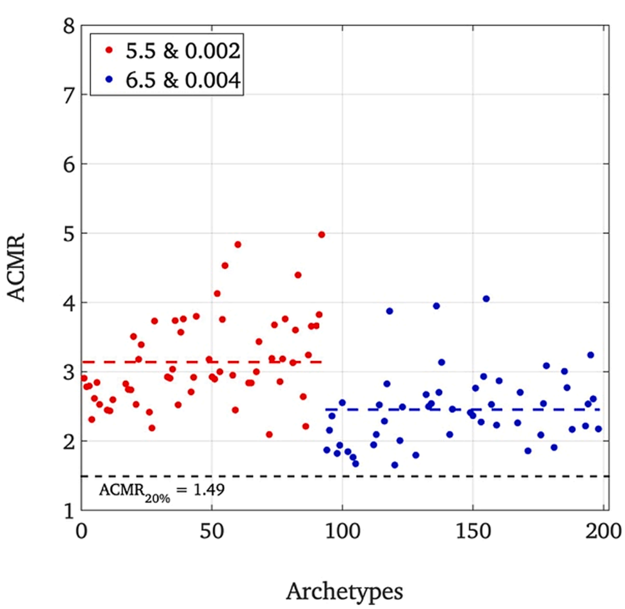

Fig. 14. ACMR results for the archetype set after removing the data for the cases where the structural design was controlled by the C_{min} requirement.

damage after frequent events, minimizing repair costs and maximizing the resilience of societies. Therefore, this section presents a brief analysis of the response of the 201 archetypes to different seismic demands and performance levels, aiming at providing a robust and sound framework for the validation of the new SPF set analyzed in this research.

The ASCE 41–17 standard [45] provides a set of guidelines for the perform-based evaluation and retrofit of existing and new buildings, defining three potential performance objectives for the structure under analysis: limited, basic, and enhanced. The selection of a performance objective is directly related to the extent of damage that would be sustained by the structure and its components in a seismic event, and is controlled by the acceptable damage level set by local regulations or private stakeholders. Thereby, each performance objective is quantitatively defined based on a certain combination of seismic hazard levels and building performance levels.

Seismic hazard levels aim at representing different seismic demand intensities for a particular area and are defined as spectral accelerations for a given structural period. The ASCE 41–17 standard [45] defines seismic hazard levels ranging from 50%/50 years (50% probability of exceedance in 50 years) to 2%/50 years, with discrete intervals as a function of the performance objective under evaluation. On the other hand, building performance levels are determined based on a combination of the performance of structural and non-structural elements, and are defined as discrete damage states from the infinite spectrum of possible scenarios that a structure might sustain during a seismic event. The ASCE 41–17 standard [45] lists four performance levels: operational (very light overall damage), immediate occupancy (light), life safety (moderate), and collapse prevention (severe). For a given structural system, performance levels are usually associated with an engineering demand parameter (such as interstory drift, settlement, plastic rotation, residual strength, among others) to enable a straightforward evaluation of the fulfillment of the performance level. Regarding wood frame structures, the FEMA 356 pre-standard [46] defines interstory drift limits for three performance levels: 1% for immediate occupancy, 2% for life safety, and 3% for collapse prevention. For the operational level, previous experimental research showed that a 0.6% drift [47,48] satisfies its performance requirements as outlined by the ASCE 41–17 standard [45].

For the evaluation of the archetypes presented in this research, the enhanced performance objective was selected since it seeks to guarantee the proper behavior of a structure across a wide range of seismic scenarios, evaluating low-damage states for service-level earthquakes and near-collapse scenarios for rare earthquakes. According to the ASCE 41–17 standard [45], one of the ways for a building to reach the enhanced operational objective is meeting the following: (1) fulfill either the operational or immediate occupancy performance level for a 50%/50 years seismic demand, (2) fulfill the life safety performance level for a 20%/50 years seismic demand, and (3) fulfill the collapse prevention performance level for a 5%/50 years seismic demand. These three scenarios were analyzed for the 201 archetypes of this research, and results are presented in Fig. 15.

Fig. 15(a) shows the interstory drifts expected for a 50%/50 years seismic hazard, computed as the 84th percentile values from the IDA analyses presented in Section 2.6. Fig. 15(b) and 15(c) shows the expected drifts for a 20%/50 years and 5%/50 years seismic hazard, respectively. The spectral accelerations for each seismic hazard level were extrapolated from the NCh433 design spectra [3] based on the recommendations provided by [49,50]. Results show that both SPF sets accomplish the requirements for the enhanced performance objective under the three specified seismic hazards, meeting the drift limits for each archetype in the set. Just one archetype slightly fails the operational limit for the 50%/50 hazards; however, this does not affect the overall statistical suitability of the SPFs under analysis. These results highlight that a change towards less conservative SPFs for wood frame buildings does not have a harmful effect on the seismic response of the

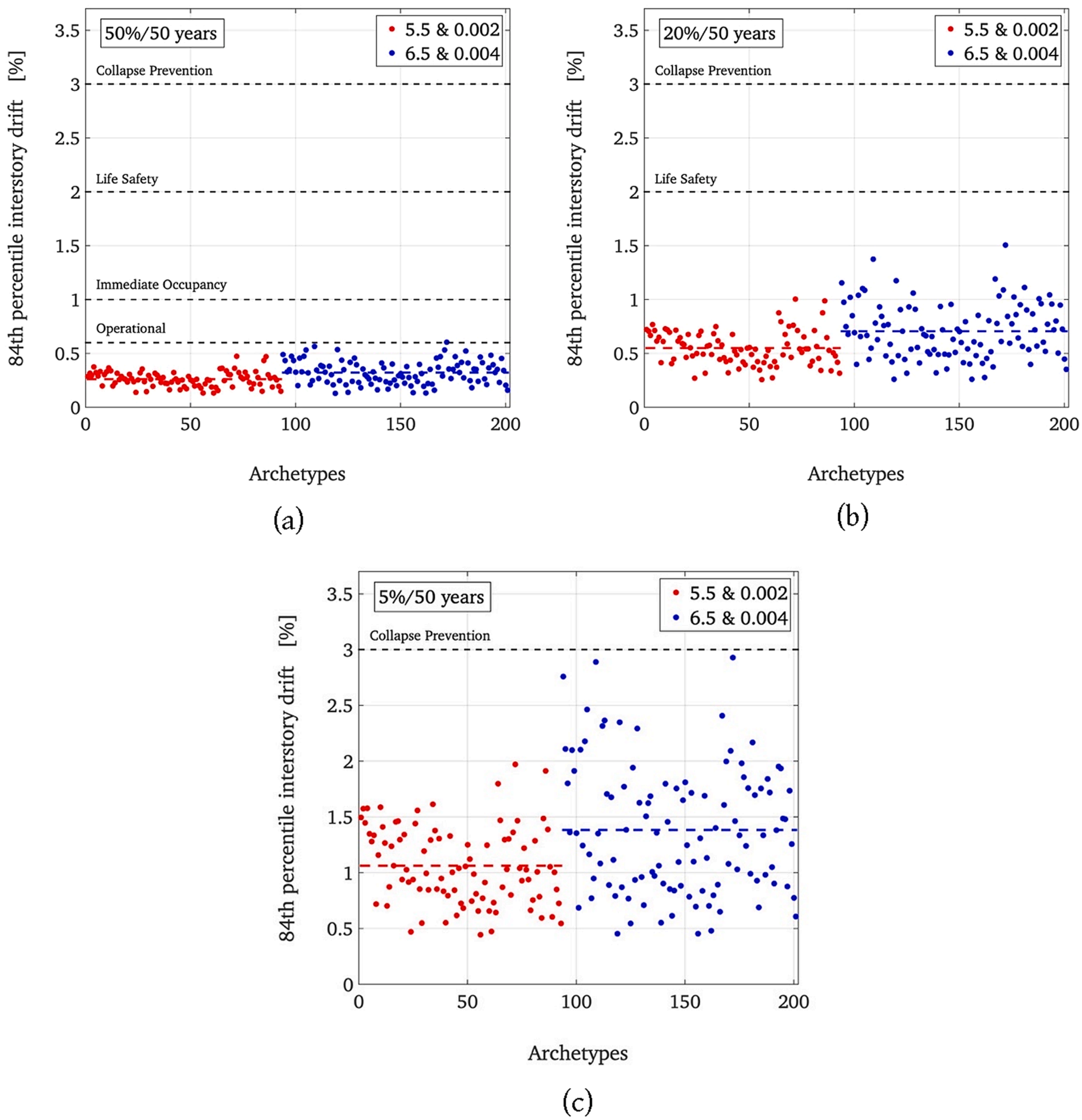

Fig. 15. 84 percentile interstory drift of the 201 archetypes under analysis for different seismic hazards: (a) 50%/50 years, (b) 20%/50 years, and (c) 5%/50 years. The dashed lines mark the drift limits for different performance levels.

structures, proving a resilient behavior under different levels of seismic hazard. Results in Fig. 15(a) are significant to show that, even if the overall stiffness of the structure is reduced due to a change in the maximum allowable story drift Δ_{max} from 0.002 to 0.004, an operational performance level can be expected for low seismic demands. This is important in the Chilean context since several minor earthquakes are expected throughout the lifespan of buildings, and SPFs should guarantee no structural and non-structural issues under highly recurring seismic events.

3.3. Collapse story analysis

Previous research has reported that wood frame buildings are prone to sustain soft-story failure modes [51,52] under moderate to severe earthquakes. This is mainly due to the presence of garage lines or wide entrance doors that weaken the capacity of first stories and concentrate the lateral deformations on the ground story walls, even if a proper procedure was followed for structural design. However, this phenomenon is not only due to the architectural configuration of the building, but also to the inherent dynamic response of the structure under lateral accelerations. For multi-story buildings, ground-level stories have a larger seismic mass on top of them compared to upper stories, resulting in high lateral displacements due to the inertial forces caused by lateral accelerations. This basic concept of structural dynamics is applicable even if the architectural configuration is the same across all stories in the building, increasing the demand/capacity ratio for lower stories. In order to analyze the extent of this phenomenon, the response-history results of the 201 archetypes of this research were analyzed to find out which stories reached the collapse drift (3%) first during the dynamic analyses, and overall results are presented in Fig. 16. It is important to highlight that all architectural configurations showed in Fig. 7 had the same wall distribution across all levels, although the strength at each story varied in proportion to design demand.

Fig. 16 shows that in 57% of cases the first story reached the collapse

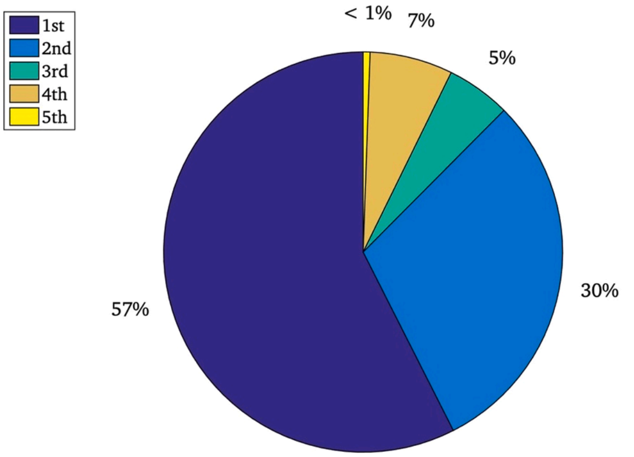

Fig. 16. Collapse story percentages for the 201 archetypes analyzed in this research.

drift first, in 30% the second story, and in the remaining cases the upper levels (in 5%, 7%, and <1% of cases, the third, fourth, and fifth story, respectively). No case showed a collapse on the sixth story. Interestingly, it can be noted that 87% of the analyses collapsed on the ground stories due to the increased seismic forces at the ground levels regardless of their architectural configuration. Fig. 17 shows the collapse levels classified by the number of stories of the archetype. Results show the same trend discussed above for all archetype heights, with most collapses occurring on the first and second stories. However, it is interesting to note that for the five- and six-story buildings, a significant amount of cases (12% and 28%) collapsed on the fourth story. This may be explained due to the fact that as the height of the structure increases, its modal shapes change and higher modes of vibrations become significant, affecting the overall response of the structure. However, the collapse percentages on the lower stories for those archetypes are still high, with 79% and 51% of the cases collapsing on the first two levels for the five- and six-story archetypes, respectively. Several mechanisms could be implemented into wood frame structures to mitigate this phenomenon and enhance the response of the building, such as stiffening of the first stories with higher capacity materials (such as steel frames), incorporating seismic dampers at critical levels, or installing base isolators at the ground story to reduce the seismic energy input to the structure. Further research should investigate the suitability and cost-effectiveness of these approaches.

4. Conclusions

This paper presents the results of an experimental and numerical investigation on the seismic performance factors (SPF) for wood frame buildings in Chile. Since previous research has shown that the current provisions of the Chilean NCh433 standard [3] result in over-conservative structures, the main goal of this research is to propose a new set of SPFs in order to improve the cost-effectiveness of new buildings without compromising their seismic response. Following the guidelines of the FEMA P-695 methodology [1] and a new ground motion set proposed for subduction zones, 201 structural archetypes were analyzed through nonlinear numerical models to study their dynamic behavior under different seismic hazards. The archetypes assessed two different sets of SPFs: (1) the current provision of the NCh433 standard, $R = 5.5$ & $\Delta_{max} = 0.002$, and (2) a new set of less conservative SPFs, $R = 6.5$ & $\Delta_{max} = 0.004$. Results showed that the new proposed set results in code-compliant structures with an acceptably low probability of collapse under maximum considered earthquake MCE accelerations. Besides, the structural efficiency improves, more flexible architectural designs are allowed, and the resilience of the buildings is guaranteed even for highly recurring seismic events. The main findings of this research are as follows:

- At the individual level, when the SPFs were changed from $R = 5.5$ & $\Delta_{max} = 0.002$ to $R = 6.5$ & $\Delta_{max} = 0.004$ the average collapse margin ratio of the archetypes reduced by 13.3%. However, no archetype

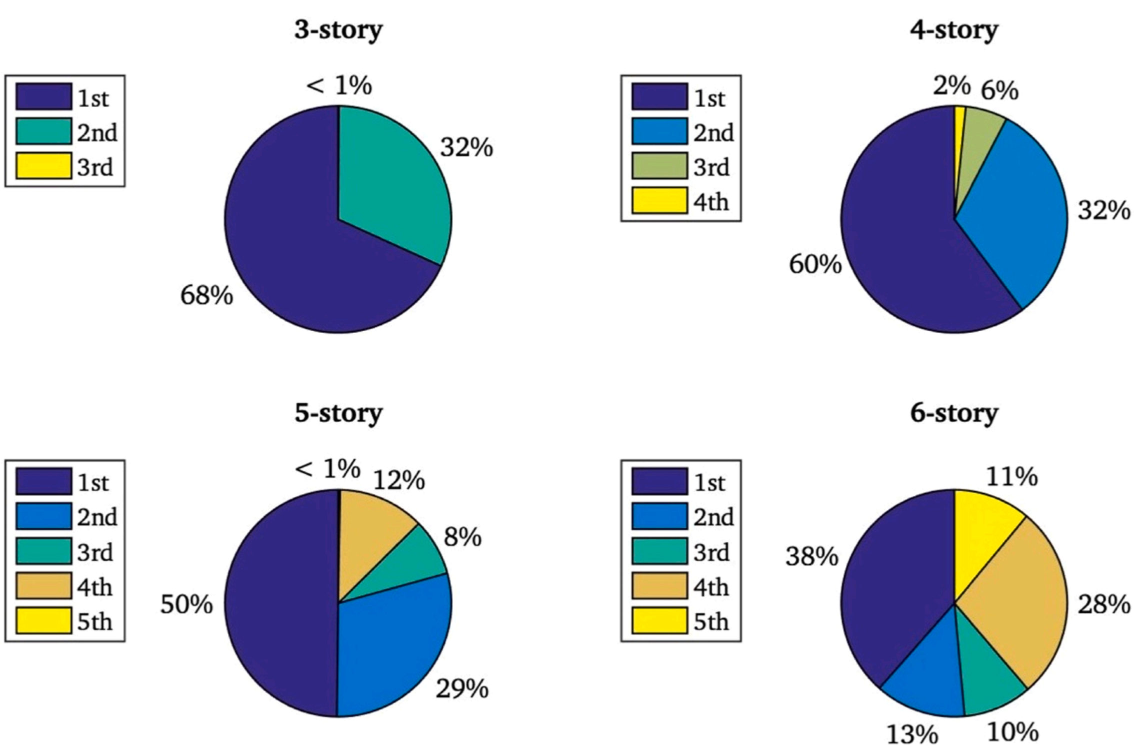

Fig. 17. Collapse story percentages classified by building height.

showed a collapse probability higher than 20% for MCE accelerations.

- At the group level, when the SPFs were changed from R = 5.5 & Δ_{max} = 0.002 to R = 6.5 & Δ_{max} = 0.004, the average collapse margin ratio of the performance groups reduced by 15.3%. However, no group showed a collapse probability higher than 10% for MCE accelerations.
- Employing less conservative SPFs improves the cost-effectiveness ratio of wood frame structures and might enhance its competitiveness when compared to other materials. For instance, the new set of SPFs resulted in a 40.4% saving in nailing, 15.9% in OSB panels, and 7.3% in timber studs for a 5-story building case study.
- For wood frame structures, the building height proved not to have a relevant influence on the seismic behavior of the structure, since similar collapse ratios were found for archetypes with a different number of stories.
- The minimum base shear requirement C_{min} of the NCh433 standard is somewhat restrictive for soil classes A, B, and C, leading to conservative results compared to archetypes where the minimum base shear C_{min} does not control the structural design. However, the conservatism of the C_{min} value is due to the inherent uncertainty of the seismic hazard, and aims at providing a design base shear high enough to guarantee the resilience of the structures under moderate and severe earthquakes.
- Wood frame structures designed with the current SPFs of the NCh433 standard or the new SPFs proposed in this research proved to meet the enhanced performance objective defined by the ASCE 41–17 standard. This highlights that a change towards less conservative SPFs for wood frame buildings does not have a harmful effect on the seismic response of the buildings.
- A reduction in the overall stiffness of wood frame structures due to a change in the maximum allowable drift Δ_{max} from 0.002 to 0.004 does not prevent the buildings from reaching an operational performance level for low seismic demands. This is important in the Chilean context since several minor earthquakes are expected throughout the lifespan of buildings, and SPFs should guarantee no structural and non-structural issues under highly recurring seismic events.
- Due to the higher seismic mass on top of ground-level floors and the consequent increased demand/capacity ratio, lower stories sustain higher lateral displacements and are more likely to collapse under lateral accelerations compared to the upper floors. This is valid even if no garage lines or wide entrance doors are part of the architectural design of the first floor. In this research, it was found that 87% of the archetypes under analysis collapsed on the first and second floor regardless of the SPF set used during design.

CRediT authorship contribution statement

Xavier Estrella: Conceptualization, Investigation, Methodology, Software, Writing – original draft, Writing – review & editing. **Pablo Guindos:** Conceptualization, Resources, Methodology, Writing – review & editing. **José Luis Almazán:** Conceptualization, Supervision, Methodology, Supervision, Writing – review & editing. **Sardar Malek:** Conceptualization, Methodology, Formal analysis, Supervision, Writing – review & editing. **Hernán Santa María:** Conceptualization, Methodology, Resources, Funding acquisition, Project administration, Writing – review & editing. **Jairo Montaño:** Conceptualization, Methodology, Writing – review & editing. **Sebastián Berwart:** Conceptualization, Methodology, Writing – review & editing.

Declaration of Competing Interest

The authors declare that they have no known competing financial interests or personal relationships that could have appeared to influence the work reported in this paper.

Acknowledgements

The funding for this research was provided by ANID (Doctorado Nacional 2019 - 21191267), Graduate Research School UTS, VRI UC, and the Research Center for Integrated Disaster Risk Management (CIGIDEN), ANID/FONDAP/1511001. The authors thank Simpson Strong-Tie Company for the donation of anchorages and connectors and its valuable financial support to this investigation.

References

[1] FEMA. Quantification of building seismic performance factors. Federal Emergency Management Agency, Washington, D.C.; 2009.
[2] Baker W, Besjak C, Sarkisian M, Lee P, Doo C. Proposed methodology to determine seismic performance factors for steel diagrid framed systems. Chicago, Illinois: Council on Tall Buildings and Urban Habitat; 2010.
[3] INN. Diseño sísmico de edificios. NCh 433.Of1996Mod2012. Santiago, Chile: Instituto Nacional de Normalización; 2009.
[4] ASCE. Minimum design loads and associated criteria for buildings and other structures. ASCE Standard ASCE/SEI 7-16. Reston, Virginia: American Society of Civil Engineers; 2016.
[5] Dolan D, Dechent P, Giuliano G. Comparison of Chilean and US seismic design provisions for timber structures. In 51st Int. Conv. Soc. Wood Sci. Technol., Concepcion, Chile; 2008.
[6] Santa María H, Caicedo N, Montaño J, Almazán J. Towards timber mid-rise buildings in Chile: structural design challenge and regulation gaps. In Proc. WCTE 2016 World Conf. Timber Eng., Vienna, Austria; 2016.
[7] Cárcamo S, Caamaño J, Cid A. Diseño interdisciplinario para el sistema constructivo marco y plataforma, recomendaciones para una buena estructuración. Buenos Aires, Argentina: CLEM-CIMAD; 2017.
[8] Guíñez F, Santa María H, Almazán JL. Monotonic and cyclic behaviour of wood frame shear walls for mid-height timber buildings. Eng Struct 2019;189:100–10. https://doi.org/10.1016/J.ENGSTRUCT.2019.03.043.
[9] Dechent P, Silva R, Dolan D, Giuliano G, Crempien J, Matamala J. Simplified design seismic-resistant method for low-rise light-framed shear wall buildings. In 16th World Conf. Earthq. Eng., Santiago, Chile; 2017.
[10] INN. Madera estructural. Determinación de propiedades físicas y mecánicas de la madera clasificada por su resistencia. Parte 1: Métodos de ensayo en tamaño estructural. NCh 3028/1-Of 2006. Santiago, Chile: Instituto Nacional de Normalización; 2006.
[11] ASTM. ASTM D2719–13: Standard test methods for structural panels in shear through-the-thickness. West Conshohocken, PA: ASTM International; 2013.
[12] Folz B, Filiatrault A. Cyclic analysis of wood shear walls. J Struct Eng 2001;127:433–41.
[13] Segura G. Determinación del módulo de corte de tableros de fibra orientada a través de ensayo de análisis modal. Bachelor's Dissertation, Department of Civil and Environmental Engineering. Concepción, Chile: Universidad del BíoBío; 2017.
[14] Cartes S, González M, Padilla J. Actualizar tensiones basicas admisibles de madera aserrada de pino radiata para uso de elementos laminados. Concepción, Chile: Simp. Habilitación Prof; 2017.
[15] INN. Madera - Construcciones en Madera – Cálculo. NCh 1198. Santiago, Chile: Instituto Nacional de Normalización; 2014.
[16] INFOR. Ensayos de flexión, tracción y compresión a madera aserrada de Pino Radiata. Concepción, Chile: Instituto Forestal; 2017.
[17] Krawinkler H, Parisi F, Ibarra L, Ayoub A, Medina R. Development of a testing protocol for woodframe structures. CUREE Report W-02, Task 1.3.2, Consortium of. Richmond, CA: Universities for Research in Earthquake Engineering; 2001.
[18] Seim W, Kramar M, Pazlar T, Vogt T. OSB and GFB as sheathing materials for timber-framed shear walls: comparative study of seismic resistance. J Struct Eng 2016;142:E4015004. https://doi.org/10.1061/(ASCE)ST.1943-541X.0001293.
[19] Sartori T, Tomasi R. Experimental investigation on sheathing-to-framing connections in wood shear walls. Eng Struct 2013;56:2197–205. https://doi.org/10.1016/j.engstruct.2013.08.039.
[20] Casagrande D, Bezzi S, D'Arenzo G, Schwendner S, Polastri A, Seim W, et al. A methodology to determine the seismic low-cycle fatigue strength of timber connections. Constr Build Mater 2020;231:117026. https://doi.org/10.1016/j.conbuildmat.2019.117026.
[21] Jara A, Benedetti F. Informe No. 14 – Registro de estudio de ensayos de conectores. Concepción, Chile: University of the Bío Bío; 2017.
[22] American Wood Council. Special design provisions for wind and seismic. ANSI/AWC SDPWS-2015, Leesburg, VA; 2015.
[23] Estrella X, Malek S, Almazán JL, Guindos P, Santa María H. Experimental study of the effects of continuous rod hold-down anchorages on the cyclic response of wood frame shear walls. Eng Struct 2021;230:111641. https://doi.org/10.1016/j.engstruct.2020.111641.
[24] Pang W, Hassanzadeh S. Corotational model for cyclic analysis of light-frame wood shear walls and diaphragms. J Struct Eng 2012;139:1303–17. https://doi.org/10.1061/(asce)st.1943-541x.0000595.
[25] Sadeghi Marzaleh A, Nerbano S, Sebastiani Croce A, Steiger R. OSB sheathed light-frame timber shear walls with strong anchorage subjected to vertical load, bending moment, and monotonic lateral load. Eng Struct 2018;173:787–99. https://doi.org/10.1016/j.engstruct.2018.05.044.

[26] Estrella X, Guindos P, Almazán J, Malek S. Efficient nonlinear modeling of strong wood frame shear walls for mid-rise buildings. Eng Struct 2020;215:1–15.
[27] Pei S, van de Lindt J. Coupled shear-bending formulation for seismic analysis of stacked wood shear wall systems. Earthq Eng Struct Dyn 2009;38:1631–47.
[28] Pei S, van de Lindt J. Seismic numerical modeling of a six-story light-frame wood building: comparison with experiments. J Earthq Eng 2011;15:924–41. https://doi.org/10.1080/13632469.2010.544840.
[29] van de Lindt J, Pei S, Liu H, Filiatrault A. Three-dimensional seismic response of a full-scale light-frame wood building: numerical study. J Struct Eng 2010;136:56–65.
[30] Estrella X, Malek S, Almazán J, Guindos P, Santa María H. Effects of continuous rod hold-down anchors on the cyclic response of wood frame walls. Eng Struct 2020 [submitted for publication].
[31] Cárcamo S. Report N° 7 – Proposed architectural configurations. Santiago, Chile: Timber Innovation Center; 2017.
[32] Chacón M, de la Llera J, Hube M, Marques J, Lemnitzer A. Epistemic uncertainty in the seismic response of RC free-plan buildings. Eng Struct 2017;141:687–702. https://doi.org/10.1016/j.engstruct.2017.03.015.
[33] Estrella X. Report N° 24 - Numerical report of buildings seismic performance. Santiago, Chile: Timber Innovation Center; 2019.
[34] Nassani DE. A simple model for calculating the fundamental period of vibration in steel structures. APCBEE Procedia 2014;9:339–46. https://doi.org/10.1016/j.apcbee.2014.01.060.
[35] Wescott J. Horizontal stiffness of wood diaphragms. Ph.D. Dissertation, Faculty of Civil Engineering, Virginia Polytechnic. Blacksburg, VA: Institute and State University; 2005.
[36] Huang X. Diaphragm stiffness in wood-frame construction. Master Dissertation. Vancouver, Canada: Faculty of Graduate and Postdoctoral Studies, University of British Columbia; 2013.
[37] Simpson Strong-Tie. Wood construction connectors. Pleasanton, CA: Simpson Strong-Tie Company Inc; 2015.
[38] Simpson Strong-Tie. Seismic and wind anchor tiedown system guide. Canada: Simpson Strong-Tie Company Inc; 2018.
[39] Berwart S, Montaño J, Santa María H. Manual de diseño de estructuras de madera. Santiago, Chile: Centro de Innovación En Madera CIM-UC; 2020.
[40] Vamvatsikos D, Cornell C. Incremental dynamic analysis. Earthq Eng Struct Dyn 2002;31:491–514.
[41] Estrella X, Guindos P, Almazán J. Ground motions for FEMA P-695 application in subduction zones. Lat Am J Solids Struct 2019;16:1–19.
[42] Pei S, van de Lindt J. User's manual for SAPWood for Windows. Version 2.0. Fort Collins, Colorado: Colorado State University; 2010.
[43] INN. Análisis y diseño de edificios con aislación sísmica. NCh 2745-2013. Santiago, Chile: Instituto Nacional de Normalización; 2013.
[44] Estrella X. Report N° 25 - Analysis and conclusions regarding validation of the system used. Santiago, Chile: Timber Innovation Center; 2019.
[45] ASCE. Seismic evaluation and retrofit of existing buildings. ASCE Standard ASCE/SEI 41-17. Reston, Virginia: American Society of Civil Engineers; 2017.
[46] FEMA. FEMA 356: Prestandard and commentary for the seismic rehabilitation of buildings. Washington, D.C.: Federal Emergency Management Agency; 2000.
[47] van de Lindt J, Gupta R. Damage and damage prediction for wood shearwalls subjected to simulated earthquake loads. J Struct Eng 2006;20:176–84.
[48] Langlois JD, Gupta R, Miller TH. Effects of reference displacement and damage accumulation in wood shear walls. J Struct Eng 2004;130:470–9. https://doi.org/10.1061/(ASCE)0733-9445(2004)130:3(470).
[49] Guendelman T. Análisis y diseño sísmico de edificios de hormigón armado. La Serena, Chile: Universidad de La Serena; 2002.
[50] Aguiar R. Análisis sísmico por desempeño. Sangolquí, Ecuador: ESPE; 2003.
[51] ATC. Here today—Here tomorrow, earthquake safety for soft-story buildings. San Francisco, USA: Applied Technology Council, San Francisco Department of Building Inspection; 2008.
[52] van de Lindt J, Pei S, Pang W, Shirazi S. Collapse testing and analysis of a light-frame wood garage wall. J Struct Eng 2012;138:492–501. https://doi.org/10.1061/(asce)st.1943-541x.0000472.